ChemPubSoc Europe

DOI: 10.1002/cctc.201801981

CHEMCATCHEM Full Papers

Reactions of D_2 with 1,4-Bis(diphenylphosphino) butane-Stabilized Metal Nanoparticles-A Combined Gas-phase NMR, GC-MS and Solid-state NMR Study

Niels Rothermel,[a] Tobias Röther,[a] Tuğçe Ayvalı,[b, c] Luis M. Martínez-Prieto,[b] Karine Philippot,[b] Hans-Heinrich Limbach,[a, d] Bruno Chaudret,*[e] Torsten Gutmann,*[a] and Gerd Buntkowsky*[a]

The reactions of three metal nanoparticle (MNP) systems Ru/dppb, RuPt/dppb, Pt/dppb (dppb = 1,4-bis(diphenylphosphino)-butane) with gaseous D_2 at room temperature and different gas pressures have been studied using ^{1}H gas phase NMR, GC-MS and solid state ^{13}C and ^{31}P MAS NMR. The main product is gaseous HD arising from the reaction of D_2 with surface hydrogen sites created during the synthesis of the nanoparticles. In a side reaction, some of the dppb ligands are decomposed producing surface phosphorus species and gaseous partially deuterated butane and cyclohexane. These findings are fundamental for detailed studies of the reaction kinetics of these particles towards H_2 or D_2 gas.

Introduction

Nanoparticles of transition metals, stabilized by organic ligands, are an interesting class of catalysts, since they represent a hybrid between a heterogeneous and a homogeneous catalyst. The combination of both fields is important for hydrogenations of arenes under mild conditions.[1] In comparison to classical heterogeneous catalysts, such as zeolite-supported noble metals used for aromatic hydrogenations,[2] metal nanoparticles offer many possibilities for fine tuning with respect to activity and selectivity due to their stabilizing ligand system. This makes it possible to modify nanoparticles not only for operations in different solvents such as aromatics, alcohols and even water, but also for stereoselective operations.[3] Particles tuned in this way have been recently used for the regioselective and stereo specific deuteration of a wide range of bioactive aza compounds.[4]

To design metal nanoparticle systems that fulfill the high demands on activity and selectivity of modern catalysis, it is crucial to gain a deeper understanding of the processes that take place on the nanoparticle surface during the catalytic reaction. For the characterization of surface species and the observation of surface processes on metal nanoparticles (MNPs), solid state and gas phase NMR have proven to be valuable spectroscopic methods.[5] For MNPs formed by hydrogenation of organometallic precursors it has been shown by a combination of ^{1}H gas phase and solid state ^{2}H NMR that hydrides are present on the surface of the particles and that they are mobile and exchangeable by deuterium.[6] Recently, some of us have explored the kinetics of gas-solid hydrogen isotope exchange of ruthenium metal nanoparticles (RuMNPs) in more detail.[7] It was found that when D_2 is applied to RuMNPs, a direct reaction with surface hydrides occurs without D_2 dissociation leading to the formation of HD in the initial reaction stages.

Whereas we have studied previously RuMNPs containing different stabilizing ligand systems, namely Ru/PVP (PVP = polyvinylpyrrolidone) and Ru/HDA (HDA = hexadecylamine), we have investigated in the present work the more reactive Ru/dppb system (**1**) (dppb = 1,4-bis(diphenylphosphino)butane) at 1 and 2 bar D_2 pressures. As we also wanted to explore the role of the metal, we extended our work to the bimetallic system of ruthenium and platinum RuPt/dppb (**2**). In such bimetallic systems, the presence of the second metal is assumed to tune the binding properties of the hydrogen.[8] Finally, the monometallic system of platinum Pt/dppb (**3**) is investigated. In the course of our studies, we observed a hydrogenation of the phenyl groups of dppb and a partial decomposition of the ligand system that leaves into the gas phase. Therefore, the composition of the gas phase has been further analyzed in detail by GC-MS. Finally, multinuclear solid-state NMR experi-

[a] N. Rothermel, T. Röther, Prof. Dr. H.-H. Limbach, Dr. T. Gutmann, Prof. Dr. G. Buntkowsky
TU Darmstadt
Eduard-Zintl-Institut für Anorganische und Physikalische Chemie
Alarich-Weiss-Straße 4, 64287 Darmstadt (Germany)
E-mail: gutmann@chemie.tu-darmstadt.de
gerd.buntkowsky@chemie.tu-darmstadt.de
[b] Dr. T. Ayvalı, Dr. L. M. Martínez-Prieto, Dr. K. Philippot
LCC-CNRS Université de Toulouse; CNRS
205 Route de Narbonne, 31077 Toulouse (France)
[c] Dr. T. Ayvalı
Wolfson Catalysis Centre; Department of Chemistry
University of Oxford
Oxford OX1 3QR (UK)
[d] Prof. Dr. H.-H. Limbach
Freie Universität Berlin
Institut für Chemie und Biochemie
Takustr. 3, 14195 Berlin, (Germany)
[e] Dr. B. Chaudret
Université de Toulouse; INSA, UPS, CNRS, LPCNO
135 avenue de Rangueil, 31077 Toulouse (France)
E-mail: chaudret@insa-toulouse.fr

Supporting information for this article is available on the WWW under https://doi.org/10.1002/cctc.201801981

ments have been used to evaluate the impact of hydrogen gas on the structure of the particles' ligand shell.

Experimental Section

General

All reactions were carried out using Schlenk or Fisher-Porter bottle techniques under an inert and dry atmosphere. THF was distilled over CaH_2 and pentane over sodium. The solvents were degassed by means of three freeze-pump cycles. 1,4-bis(diphenylphosphino)-butane (dppb) was purchased from Sigma-Aldrich and [(1,5-cyclo-octadiene)(1,3,5-cyclooctatriene)ruthenium(0)] (Ru(COD)(COT)) for the synthesis of Ru/dppb (1) from Umicore. For RuPt/dppb (2) the Ru(COD)(COT) precursor was purchased from Nanomeps (Toulouse) and $Pt(CH_3)_2$(COD) from Strem. Pt/dppb (3) was synthesized using $Pt(dba)_2$ as the metal source, which was prepared according to the literature.[10] Potassium tetrachloroplatinate(II) (K_2PtCl_4) and dibenzylideneacetone (dba) were purchased from Strem Chemicals and Alfa-Aesar, respectively, and used without further purification. D_2 (99.82%) gas for the exchange reactions was purchased from Eurisotop.

Synthesis

The synthesis of all three nanoparticle systems followed the organometallic approach described in the literature,[5c,d,9] where transition metal complexes containing unsaturated ligands are hydrogenated using gaseous H_2 in dilute solutions of THF at room temperature, in the presence of a sub-stoichiometric amount of dppb.

Ru/dppb (1)

The synthesis of Ru/dppb (**1**) is described in ref.[5c] In a typical procedure, 200 mg of Ru(COD)(COT) (0.634 mmol) were introduced in a Fisher-Porter bottle and left in vacuum for 30 min. 120 mL of freshly distilled THF was then added and the resulting yellow solution was cooled to 193 K. Under rigorous stirring, a solution of 27 mg (0.0633 mmol, 0.1 eq.) dppb in 80 mL THF was slowly added to the precursor solution. The Fisher-Porter bottle was pressurized with 3 bar of H_2 gas and the solution was left to slowly reach room temperature (r.t.) under continuous stirring. After 18 h of reaction a black colloidal solution was obtained. The solvent was removed in vacuum to reach a volume of approximately 10 mL. To this solution 80 mL of pentane were added. After 1 h a black precipitate was formed and the solvent was removed by filtration. The black precipitate was further washed with 2×35 mL pentane and dried at room temperature under vacuum over night to yield Ru/dppb (**1**) particles as a black powder.

Ru/dppb NPs display a mean size of ca. 2 nm. TEM images and further characterization can be found in our previous report.[5c]

RuPt/dppb (2)

The synthesis of RuPt/dppb (**2**) is described in Ref. [9] In a typical procedure, the organometallic complexes [Ru(COD)(COT)] (189 mg, 0.601 mmol) and [Pt(CH3)2(COD)] (200 mg, 0.601 mmol) were introduced in a Fischer-Porter reactor and dissolved in 40 mL of degassed THF. The resulting yellow solution was cooled at −60 °C and a THF solution (32 ml) containing dppb (127.92 mg, 0.300 mmol) was added. After pressurizing the Fischer-Porter bottle with 3 bar of H_2, the solution was left to reach room temperature. The homogeneous solution became black after 20 min of reaction at room temperature and was kept under stirring overnight. Excess of H_2 was eliminated and the volume of solvent was reduced to 10 mL under vacuum. 40 mL of pentane were then added to the colloidal suspension, which was cooled down to −30 °C to precipitate the particles. After filtration under argon, the black solid powder was washed twice with pentane (2×40 mL) and filtrated again before drying under vacuum.

Elemental analysis yield C, 17.2%; H, 1.6% ; Ru content (ICP): 25.9% Pt content (ICP): 41%.

RuPt/dppb NPs display a mean size of ca. 1.8 nm. TEM images and further characterization can be found in our previous report.[9]

Pt/dppb (3)

The synthesis of Pt/dppb (**3**) is described in Ref. [5d] In a typical procedure, 300 mg of $Pt(dba)_2$ (0.452 mmol) were dissolved in 170 mL THF in a Fisher-Porter bottle. The obtained purple black solution was cooled to 243 K and a solution of 38.6 mg (0.0905 mmol, 0.2 eq.) dppb in 10 mL THF was added under stirring. The mixture was then pressurized with 3 bar of H_2 gas and left to slowly reach r.t. under continuous stirring. After 24 h of reaction, the black colloidal solution was reduced to a volume of approximately 20 ml in vacuum and 30 mL of cold pentane were added for a quick precipitation of a black solid. The solvent was removed by filtration and the product was further washed with 6×30 mL of cold pentane. The product was dried under vacuum overnight, yielding Pt/dppb (**3**) particles.

Pt/dppb NPs display a mean size of ca. 2 nm. TEM images and further characterization can be found in our previous report.[5d]

Characterization Techniques

Gas Phase NMR

^{1}H gas-phase NMR spectra were recorded on a Bruker Avance III HD 500 spectrometer at 11.7 T corresponding to a frequency of 500.26 MHz for ^{1}H. This system is equipped with a Bruker DUL 500 MHz S2 5 mm Probe.

10 mg of the corresponding nanoparticles (**1**–**3**) were filled into a sealable pressure resistant NMR sample tube (Wilmad Lab-Glass Quick Pressure Valve NMR Sample Tube, 2.51 mL inner volume). The sample tube was evacuated for at least 30 min before connection to a D_2 gas bottle via PFA tubing. The D_2 pressure was adjusted to 1 bar (**1 a**–**3 a**) or 2 bar (**1 b**–**3 b**), respectively, and the Teflon seal of the evacuated sample tube was opened quickly to apply a D_2 atmosphere to the particles. The tube was sealed again and directly put into the spectrometer to record ^{1}H NMR spectra of the gas phase containing an assumed mixture of H_2, HD, D_2 and volatile solvent molecules.

Gas Chromatography and Mass Spectrometry

For RuPt/dppb nanoparticles, an analysis of the gas-phase was performed by GC-MS. Experiments were performed on a Fisions

MD 800 mass spectrometer equipped with a quadrupole detector and a DB-5 column. For the measurement a sample of 12.6 mg RuPt/dppb was treated with 3 bar D_2 at r.t. (**2 c**) and stored for 7 days. The injector was heated to 240 °C and a volume of 200 μL of the gas-phase above the RuPt/dppb was injected. A temperature ramp (40 °C for 10 min, heating 25 °C/min to 150 °C, keeping 150 °C for 2 min) and He as carrier gas was chosen to separate the different side products that were analyzed by MS.

Solid State NMR

^{13}C and ^{31}P CP MAS experiments were recorded on a Bruker Avance III spectrometer at 7 T corresponding to a frequency of 75.47 MHz for ^{13}C and 121.49 MHz for ^{31}P, respectively. This system is equipped with a 4 mm H/X probe. All experiments were performed at spinning rates of 8 kHz and repetition delays of 4 s. The spectra were recorded utilizing ramped CP MAS sequences.[10] For ^{13}C and ^{31}P, contact times were set to 3 and 3.2 ms, respectively. Two sets of experiments were performed. One set was performed on the Ru/dppb particles (**1**) directly after they were synthesized. The other set was performed after treating the same sample with hydrogen gas (RuH/dppb (**1 c**)). The sample preparation constituted of three overnight treatments with 1.5 bar H_2 and two intraday treatments with 1.5 bar H_2 for 2 h. After each treatment, the sample was exposed to vacuum for at least 30 min to remove decomposition products of the ligands.

Results and Discussion

Gas Phase Measurements

Figure 1 depicts typical ^1H gas-phase NMR spectra obtained for all three particle systems after 16 h exposure to 1 bar (**1 a**–**3 a**) or 2 bar (**1 b**–**3 b**) D_2 at room temperature. All spectra show a signal at 4.5 ppm arising from gaseous dihydrogen. By line shape analysis (**1 d**, see ESI Figure S1) a line width of about 180 Hz is obtained which corresponds to the one of HD, *i.e.* the amount of H_2 is negligible as it exhibits a much broader line width (see ESI Figure S2 and Ref. [7]). This result is corroborated by the Raman spectrum (**1 e**, ESI Figure S3) recorded for the gas-phase upon reaction of D_2 with the particles, where H_2 is barely observable, in contrast to the vibrations of HD and D_2.

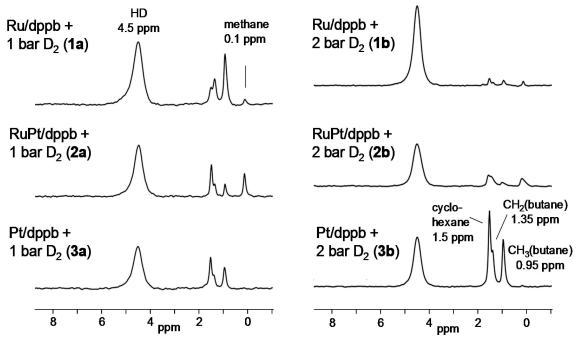

Figure 1. Typical ^1H gas-phase NMR spectra after exposing solid MNPs at room temperature to 1 bar (**1 a**–**3 a**) or 2 bar (**1 b**–**3 b**) D_2 gas for 16 h. The chemical shift of the HD signal is set to 4.5 ppm. For comparison of the signal intensities of the different particle systems, all spectra were processed using the same parameters.

In addition to HD as main reaction product, the spectra in Figure 1 reveal the formation of side products giving rise to signals at high field between 0 and 1.5 ppm. This region is typical for alkanes which must have been formed by reaction of D_2 with the dppb ligands. That reaction is corroborated for Pt/dppb sometimes by the observation of a thin film of a liquid, condensing at the inner wall of the NMR tube when the D_2 gas is applied for sample preparation. We assign these alkane signals as follows. The signal at 1.5 ppm is typical for cyclohexane[11] and those at 1.35 ppm and 0.95 ppm for the methylene and methyl groups of butane.[12] These peaks are broader as compared to the liquid state because of efficient longitudinal and transverse spin-rotation and dipolar relaxation mechanisms arising from the coherent and incoherent molecular rotation in the gas phase. This effect is stronger for small molecules such as HD, and even more pronounced for H_2.[7,13] In contrast to the Pt-containing NPs, the spectra of the Ru-containing NPs present an additional signal around 0.1 ppm. That is the chemical shift of methane.[14] From Figure 1 it is evident that the Pt and Ru containing NPs exhibit a different pressure dependence. In case of the Pt/dppb NPs, the alkane signals grow with pressure and in case of the Ru-containing NPs, the alkane signals are weakened with increasing pressure. This is a clear indication that the H/D exchange in the alkane moieties of the ligand is more efficient in the Ru/dppb NPs.

As the alkanes formed from Ru/NPs will be partially deuterated, one might expect that part of the corresponding alkane signals experience small high field shifts. Indeed, we observe in the 2 bar D_2 experiments with Ru-containing NPs that signals of the alkanes released into the gas phase contain high-field shoulders. Therefore, we checked whether these shoulders could arise from H/D isotope effects which lead to high-field shifts of the remaining carbon bound H nuclei. In the case of methane in organic solvents a high-field shift of about 0.045 ppm was observed for CH_4/CHD_3, which depended on the type of solvent and on temperature.[15] However, the shoulders which we observe seem to arise from somewhat larger shifts, their exact value being difficult to obtain. Another explanation would be that some of the alkanes at high pressure are not located in the gas phase but interacting with the particles, either adsorbed or in rapid gas-surface exchange, or as tiny droplets.

Finally, we note that in the case of RuPt/dppb the amount of obtained butane is reduced as compared to Ru/dppb, but the amount of methane increased, as expected for more efficient C–C bond breaking processes.

For the above mentioned MNPs, the alkane side products must be formed by the reaction of the dppb ligands at particularly reactive sites. The following reaction scheme is conceivable.

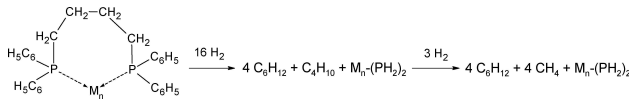

Scheme 1. Hydrogenation and alkane release of a metal dppb ligand by dihydrogen. The phosphine species formed may not be stable but subject to further reactions, in particular with oxygen.

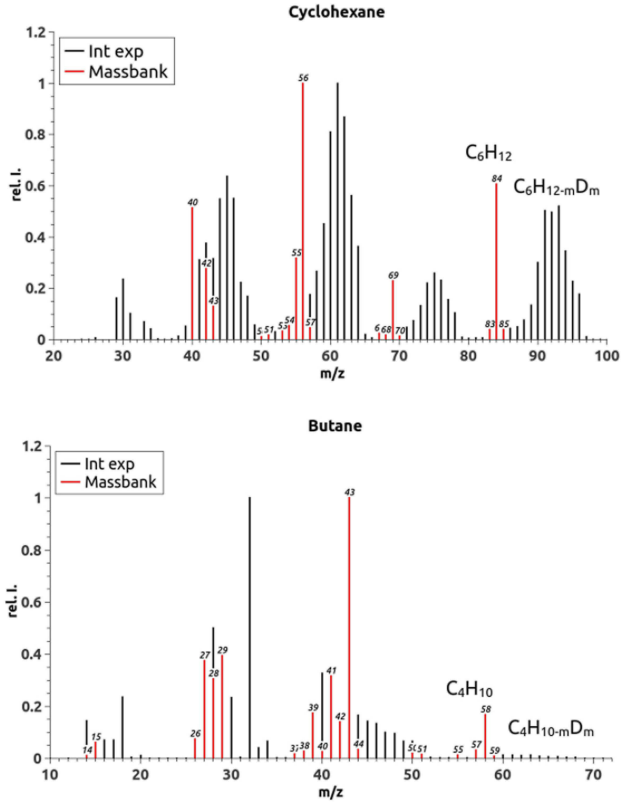

Figure 2. Recorded mass spectra of the cyclohexane and the butane fraction of the H/D exchange reaction with RuPt/dppb performed with 3 bar initial D_2 gas pressure (**2 c**). The red signals represent the mass spectrum of the individual species with natural isotope distribution as found in a mass database.

Scheme 1 suggests the formation of metal bound PH_2 surface species, but the latter might easily oxidize. In order to know the details of these reactions extended kinetic and computational studies are required which were beyond the scope of this work.

GC-MS Measurements

For the detailed characterization of the reaction products, gas-chromatography coupled to mass spectrometry (GC-MS) was applied. As an example, RuPt/dppb was treated with 3 bar D_2 gas pressure (**2 c**) to produce a higher amount of side products for analysis. RuPt/dppb (**2**) was chosen because it does not tend to quench the reaction compared to Pt/dppb (**3**) but it produces larger amounts of side product than Ru/dppb (**1**).

Two main fractions were separated (Figure 2) that are clearly attributed to cyclohexane and butane according to their spectra pattern. This is in excellent agreement with the ^1H gas phase NMRs of **1 a** and **1 b** (Figure 1), which show the signals of these compounds in the aliphatic region. The appearance of butane and cyclohexane illustrates that the particles facilitate the cleavage of the C–P bond upon decomposition of the dppb ligand, similar to related phosphido bridged transition metal cluster complexes.[16]

The spectrum of the cyclohexane fraction in Figure 2 shows a "broadening" of the mass distribution compared to the spectrum of pure cyclohexane. The location of the molecular peak at m/z = 84 is shifted to higher m/z values between 84 and 96. This is a clear hint that deuterium is incorporated into the aliphatic parts of the ligand. Similar results are also observed for the fraction of butane (Figure 2). This observation is in excellent agreement with the deuteration of alkanes on Ru/dppb MNPs as demonstrated in our previous work.[17]

Comparing the mole peak of the mass spectrum of cyclohexane and the one from butane (m/z value of 58 +), one notices a narrower distribution of masses in the case of cyclohexane and a more extensive deuteration. This phenomenon can be explained by different deuteration mechanisms. Due to the aromatic nature of the dppb ligand, some deuterons are incorporated by direct hydrogenation of the aromatic rings or already cleaved benzene.[18] This leads to the formation of cyclohexane or partly hydrogenated, respectively, deuterated C6 analogues. Furthermore, fully deuteration of the cyclohexane and C6 analogues is feasible as shown by the isotopomer patterns for the deuteration of benzene or toluene (Figure 3). This would require a C–H bond activation on the surface of the particles.

Deuteration of the butane fragment on the other hand, is only feasible through C–H-bond activation on the metal surface and not by direct reaction. Such C–H-bond activation is favored as long as the butane moiety is in close proximity to the surface which is highly probable when it is linked to phosphorus that coordinates to the surface. Based on liquid state NMR studies

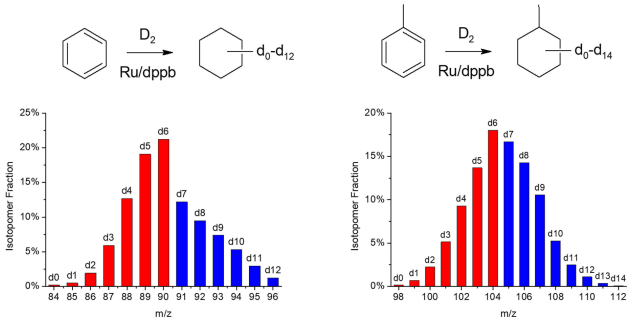

Figure 3. Isotopomer fractions obtained for the Ru/dppb catalyzed deuteration of benzene (**1 f**) and toluene (**1 g**). While the isotopomers from d_0-d_6 can be formed by hydrogenation/deuteration of the aromatic ring, for the isotopomers from d_7-d_{12} in case of cyclohexane and d_7-d_{14} in case of methylcyclohexane, a C–H bond activation on the surface of the Ru/dppb NPs is required. Note: The reactions were performed according to our previous work[17] with 6 bar D_2 gas at 60 °C. 3 batch cycles, each taking 24 h were carried out.

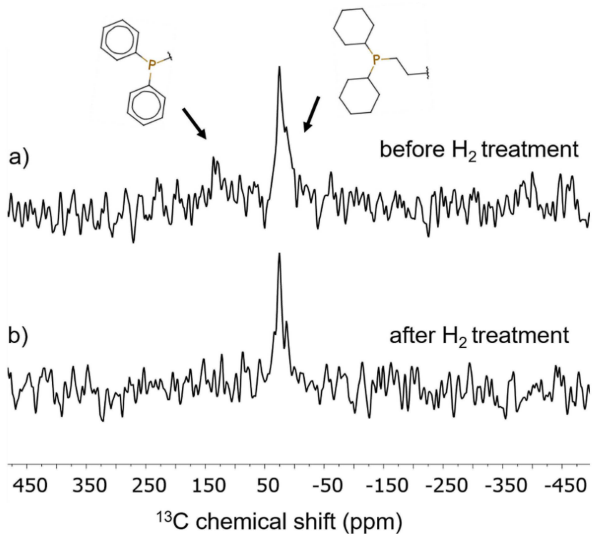

Figure 4. ^{13}C CP MAS spectra measured at 8 kHz spinning of Ru/dppb measured before (a) and after (b) treatment with H_2 gas.

on alkylamine-stabilized Ru NPs, it was previously suggested that the presence of such an agostic interaction may lead to the deuteration of alkylic species as in the present case.[5e]

Solid State NMR

The fate of the dppb ligands of Ru/dppb, RuPt/dppb and Pt/dppb was indirectly elucidated by GC-MS analysis of the side products formed when the particles are exposed to D_2 gas. The next step was to study the change of the NP surface structure, when the dppb ligand is transformed. Through the observation of cyclohexane and butane in the side product fraction, the phosphorus moieties are likely transformed into metal bound phosphanes ($-PH_xC_{3-x}$). To shed more light on the structural changes, ^{13}C and ^{31}P CP MAS NMR measurements were performed before and after hydrogen treatment (Ru/dppb (**1**) and RuH/dppb (**1 c**)).

The ^{13}C CP MAS spectra of Ru/dppb recorded before and after treatment with H_2 gas (Figure 4a,b) both feature signals of aliphatic carbons located around 25 ppm. Before the treatment, a tiny signal at 130 ppm is visible that is attributed to phenyl groups of non-hydrogenated dppb ligands. This weak aromatic signal in dppb based particles varies in intensity between different particle samples. The intensity can for example be affected by storage time and also by small experimental deviations. In addition to that, the measurement shows that not all ligands on the metal surface undergo decomposition but all aromatic species are hydrogenated. Ligands that undergo decomposition could therefore be located at very reactive sites on the metal surface. Based on previous surface studies with CO adsorbed on Ru/dppb it is assumed that ligands are located on apexes of the particle.[9] The observed decomposition products most probably stem from ligands which are not located on apex positions and are therefore labile and readily react with hydrides in their vicinity.

The ^{31}P CP MAS spectra of Ru/dppb recorded before and after treatment with H_2 gas (Figure 5a,b), show clear differences in their line shape and an improved resolution and S/N ratio is obtained after H_2 treatment. The better resolution and S/N ratio seem to be the consequence of the saturation of the metal surface with hydrogen upon H_2 treatment, which improves the cross-polarization efficiency. Nevertheless, no additional signals appeared after treatment with H_2 gas, which indicates that no significant changes of the structure occurred during the H_2 treatment.

An assignment of individual signals has to be done with care. Following previous ^{31}P solid state NMR studies[18a] the major signal located at 56 ppm is most probably attributed to phosphine species coordinated to the metal surface. Based on the characterization of the dppb chemistry towards decomposition and hydrogenation, a range of different phosphine species is expected to be present on the surface, i.e. *alkyl*-P(Ph/Cy)$_2$, *alkyl*-P(Ph/Cy)H, *alkyl*-PH$_2$, H$_n$P(Ph/Cy)$_{3-n}$ and arene hydrogenation products from all these species, which are not fully hydrogenated to cyclohexyl. Based on the ^{13}C spectra it can be assumed that arene phosphines are the least dominant surface species. The signal located at 29 ppm seems to correspond to co-adsorbed phosphine oxides.

Reactions on dppb Stabilized Nanoparticles

The results of the previous sections reveal a clearer picture on the surface reactions of dppb stabilized MNPs. For the details of the formal reactions of the dppb ligands with H_2 or D_2 (Scheme 1) we discuss some possible mechanisms depicted in Figure 6. Gaseous H_2 or D_2 are consumed and as main products butane and cyclohexane are formed as proven by NMR and GC-MS analysis of the gas phase. On the other hand, some dppb ligands remain as partially hydrogenated/deuterated ligands on the surface as evidenced by ^{13}C and ^{31}P solid-state NMR.

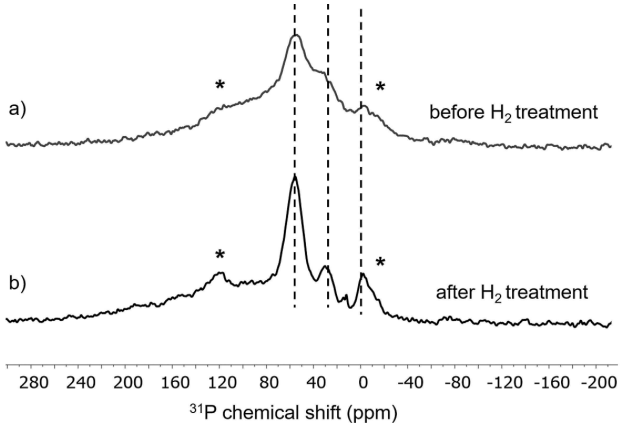

Figure 5. ^{31}P CP MAS spectra measured at 8 kHz spinning of Ru/dppb measured before (a) and after (b) treatment with H_2 gas. Note that signals marked with asterisks are spinning sidebands of the signal at ca. 56 ppm.

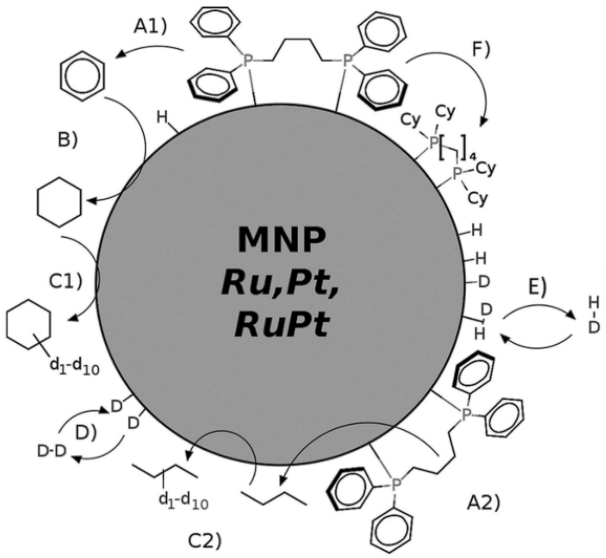

Figure 6. Reactions taking place on dppb stabilized nanoparticles when exposed to D_2.

Together with the results from our former paper on alkane deuteration[17] a variety of side reactions can be identified as illustrated in Figure 6. The reaction steps A1 and A2 describe the C–P bond cleavage catalyzed by the particle that leads to the formation of benzene and butane. The details of these complex reaction steps are illustrated in Figure S4 in the ESI. In step B, benzene reacts further to form cyclohexane. In step C1 and C2, cyclohexane or butane are deuterated by C–H bond activation on the particle surface. In addition to the reactions that involve the dppb ligand, D_2 is adsorbed on the surface and is transformed into surface deuterides in step D. Surface deuterides scramble with surface hydrides and form HD that can leave the particle due to the surface/gas phase equilibrium in step E. Finally, in a step F the hydrogenation of the dppb is feasible which leads to 1,4-*Bis*(dicyclohexylphosphino)butane in case of total hydrogenation.

Conclusions

Three 1,4-Bis(diphenylphosphino)butane stabilized nanoparticle systems (Ru/dppb, Pt/dppb and RuPt/dppb) were investigated in the reaction with D_2 gas. Next to HD exchange with gaseous dihydrogen isotopomers, these particle systems were found to be capable of catalyzing the deuteration of aliphatic substrates. The latter was confirmed by GC-MS analysis of the gas phase after reaction with D_2 gas, which allowed a detailed characterization of the side products that were observed in the ^{1}H gas phase NMR spectra. The formation of deuterated butane and cyclohexane isotopomers revealed that all three particle systems not only catalyze an isotope exchange but also catalyze P–C bond cleavage reactions of their dppb ligands in very mild reaction conditions. Exemplary, ^{13}C and ^{31}P solid state NMR experiments on Ru/dppb show that even after multiple hydrogen treatments, which trigger the decomposition of the dppb ligand, the latter remains on the particle surface. These results demonstrate that the surface composition is not drastically influenced by this decomposition reaction. For deeper studies of HD exchange kinetics, it is however necessary to pretreat the particles with H_2 gas to gain reproducible initial conditions for the surface reaction.

Acknowledgements

This research was supported by the Deutsche Forschungsgemeinschaft under contract Bu-911-19-1/2 (DFG-ANR project MOCA-NANO): The authors thank Christiane Rudolph, Gül Sahinalp and Alexander Schießer of the mass spectrometry department of TU Darmstadt for their technical support.

Conflict of interest

The authors declare no conflict of interest.

Keywords: CH-activation · Gas Phase NMR · Solid-state NMR · HD-exchange · transition metal nanoparticles

[1] a) P.-J. Debouttière, Y. Coppel, A. Denicourt-Nowicki, A. Roucoux, B. Chaudret, K. Philippot, *Eur. J. Inorg. Chem.* **2012**, 1229–1236; b) J. A. Widegren, R. G. Finke, *J. Mol. Catal. A* **2003**, *191*, 187–207.
[2] A. Stanislaus, B. H. Cooper, *Catal. Rev.* **1994**, *36*, 75–123.
[3] S. Jansat, D. Picurelli, K. Pelzer, K. Philippot, M. Gómez, G. Muller, P. Lecante, B. Chaudret, *New J. Chem.* **2006**, *30*, 115–122.
[4] a) G. Pieters, C. Taglang, E. Bonnefille, T. Gutmann, C. Puente, J.-C. Berthet, C. Dugave, B. Chaudret, B. Rousseau, *Angew. Chem. Int. Ed.* **2014**, *53*, 230–234; *Angew. Chem.* **2014**, *126*, 234–238; b) C. Taglang, L. M. Martinez-Prieto, I. del Rosal, L. Maron, R. Poteau, K. Philippot, B. Chaudret, S. Perato, A. S. Lone, C. Puente, C. Dugave, B. Rousseau, G. Pieters, *Angew. Chem. Int. Ed.* **2015**, *54*, 10474–10477; *Angew. Chem.* **2015**, *127*, 10620–10623.
[5] a) T. Gutmann, I. Del Rosal, B. Chaudret, R. Poteau, H.-H. Limbach, G. Buntkowsky, *ChemPhysChem* **2013**, *14*, 3026–3033; b) T. Gutmann, A. Grünberg, N. Rothermel, M. Werner, M. Srour, S. Abdulhussain, S. Tan, Y. Xu, H. Breitzke, G. Buntkowsky, *Solid State Nucl. Magn. Reson.* **2013**, *55–56*, 1–11; c) F. Novio, K. Philippot, B. Chaudret, *Catal. Lett.* **2010**, *140*, 1–7; d) S. Kinayyigit, P. Lara, P. Lecante, K. Philippot, B. Chaudret, *Nanoscale* **2014**, *6*, 539–546; e) C. Pan, K. Pelzer, K. Philippot, B. Chaudret, F. Dassenoy, P. Lecante, M. J. Casanove, *J. Am. Chem. Soc.* **2001**, *123*, 7584–7593.
[6] T. Pery, K. Pelzer, G. Buntkowsky, K. Philippot, H.-H. Limbach, B. Chaudret, *ChemPhysChem* **2005**, *6*, 605–607.
[7] H.-H. Limbach, T. Pery, N. Rothermel, B. Chaudret, T. Gutmann, G. Buntkowsky, *Phys. Chem. Chem. Phys.* **2018**, *20*, 10697–10712.
[8] a) L. Luo, Z. Duan, H. Li, J. Kim, G. Henkelman, R. M. Crooks, *J. Am. Chem. Soc.* **2017**, *139*, 5538–5546; b) H. Li, K. Shin, G. Henkelman, *J. Chem. Phys.* **2018**, *149*, 174705.
[9] P. Lara, T. Ayvalı, M.-J. Casanove, P. Lecante, A. Mayoral, P.-F. Fazzini, K. Philippot, B. Chaudret, *Dalton Trans.* **2013**, *42*, 372–382.
[10] G. Metz, X. L. Wu, S. O. Smith, *J. Magn. Reson. Ser. A* **1994**, *110*, 219–227.
[11] B. D. Ross, N. S. True, *J. Am. Chem. Soc.* **1983**, *105*, 4871–4875.
[12] T. Tynkkynen, T. Hassinen, M. Tiainen, P. Soininen, R. Laatikainen, *Magn. Reson. Chem.* **2012**, *50*, 598–607.
[13] A. Abragam, *The Principles of Nuclear Magnetism, Chapter VIII*, Oxford University Press, London, **1961**.
[14] G. R. Fulmer, A. J. M. Miller, N. H. Sherden, H. E. Gottlieb, A. Nudelman, B. M. Stoltz, J. E. Bercaw, K. I. Goldberg, *Organomet. Chem.* **2010**, *29*, 2176–2179.

[15] F. A. L. Anet, D. J. Oleary, *Tetrahedron Lett.* **1989**, *30*, 2755–2758.
[16] a) P. E. Garrou, *Chem. Rev.* **1985**, *85*, 171–185; b) S. A. Maclaughlin, A. J. Carty, N. J. Taylor, *Can. J. Chem.* **1982**, *60*, 87–90; c) W. H. Watson, G. Wu, M. G. Richmond, *Organomet. Chem.* **2006**, *25*, 930–945.
[17] N. Rothermel, D. Bouzouita, T. Roether, I. de Rosal, S. Tricard, R. Poteau, T. Gutmann, H. H. Limbach, B. Chaudret, G. Buntkowsky, *ChemCatChem* **2018**, *10*, 4243–4247.
[18] a) T. Gutmann, E. Bonnefille, H. Breitzke, P.-J. Debouttière, K. Philippot, R. Poteau, G. Buntkowsky, B. Chaudret, *Phys. Chem. Chem. Phys.* **2013**, *15*, 17383–17394; b) P. Lara, K. Philippot, B. Chaudret, *ChemCatChem* **2013**, *5*, 28–45; c) E. Rafter, T. Gutmann, F. Loew, G. Buntkowsky, K. Philippot, B. Chaudret, P. W. N. M. van Leeuwen, *Catal. Sci. Technol.* **2013**, *3*, 595–599.

Manuscript received: December 5, 2018
Revised manuscript received: January 15, 2019
Accepted manuscript online: January 16, 2019
Version of record online: February 13, 2019